NUMERICAL SIMULATION OF NO_X AND CO FORMATION IN NATURAL GAS DIFFUSIVE FLAMES

André A. Isnard
Departamento de Engenharia Mecânica, PUC-Rio
22453-900, Rio de Janeiro, RJ, BRAZIL
Marcos S. P. Gomes
Departamento de Engenharia Mecânica, PUC-Rio
22453-900, Rio de Janeiro, RJ, BRAZIL

Abstract. *The present paper describes a continuation of the work presented in* Isnard & Gomes (1998)*, which included the numerical modeling of the natural gas combustion and the NO_x formation process by considering the Zeldovich mechanism. Additionally, in this work it was investigated the carbon monoxide (CO) formation using a more detailed combustion model. The numerical procedure based on the finite volume formulation included the k-ε turbulence model, the generalized finite rate model of Arrhenius and Magnussen for the combustion calculations and the discrete transfer radiation model. The main goal of the inquiry was to investigate the performance of such modeling approach in predicting NO_x and CO formation and to evaluate the influence of the CO formation in the temperature field inside the furnace. The comparisons between numerical and experimental results indicated a clear evolution of the model regarding the prediction of the temperature field, species concentrations and a reasonable agreement with the NO_x formation trend.*

Key-words: *Combustion Modeling, NO_x, Natural Gas*

1. INTRODUCTION

Nitrogen oxides, recalled to as NO_x, are partially responsible for environmental damages including the photochemical smog, illness in organisms, corrosion of metals, textiles weakening and reducing the growth of vegetation. In flames, NO (nitric oxide) is the dominant component, corresponding to about 95% of all NO_x produced. The carbon monoxide (CO) is another pollutant responsible for damages to life in general. The presence of CO reduces the total capability of blood in transporting oxygen to cells.

In this work, it was investigated the performance of a model for simulating the combustion process in a pilot scale furnace. It was based on the finite volume formulation including the k-ε model of turbulence, the generalized finite rate model of Arrhenius and Magnussen for the combustion calculations and the discrete transfer radiation model. Natural gas was employed as the fuel and the Zeldovich mechanism was adopted for simulating the NO_x formation, which includes the assumption of a chemical equilibrium for estimating the [O] radical (monatomic oxygen) concentration, named here as $[O]_{equil}$. The combustion

process was represented by a two step reaction mechanism, which made it possible to predict the CO formation. The purposes of the research were: (i) to investigate the performance of this modeling approach in predicting NO_x and CO formation in natural gas industrial flames, and (ii) to identify the influence of the CO formation in the temperature field along the furnace, such that the model could then be used for evaluating the environmental impacts of various combustion equipment. The present work is a continuation of what was presented in Isnard & Gomes (1998), which included the same models employed in the present one, except for that: (i) it comprised an one step reaction combustion mechanism, (ii) it did not include the assumption of a chemical equilibrium for estimating the [O] radical concentration and (iii) it was simulated for a different geometry.

1.1 Zeldovich Mechanism of NO Formation

Zeldovich (1946) found that the nitric oxide may not be formed through direct collisions of N_2 and O_2 molecules as presented by the global reaction (1). In this manner he proposed a two reactions mechanism represented by reactions (2) and (3). This mechanism is initiated by reaction (4), which represents the dissociation of molecular oxygen, in which M denotes a third body. M may be regarded as any species such as N_2, N, NO, O_2 or O, with the function of stabilizing the reaction.

$$N_2 + O_2 \overset{k_{1f}}{\underset{k_{1b}}{=}} 2NO \tag{1}$$

$$N_2 + O \overset{k_{2f}}{\underset{k_{2b}}{=}} NO + N \tag{2}$$

$$N + O_2 \overset{k_{3f}}{\underset{k_{3b}}{=}} NO + O \tag{3}$$

$$O_2 + M \overset{k_{4f}}{\underset{k_{4b}}{=}} O + O + M \tag{4}$$

In this mechanism proposed by Zeldovich, the combustion reaction serves only as a source of energy for the reactants, as the reactions (2) and (3) occur independently of the combustion reaction. It also recommends that the NO formation rates may be calculated assuming equilibrium values for the temperature and for the concentration of O, N_2 and O_2. This procedure has been named by Zeldovich as a thermal mechanism.

2. MODEL DESCRIPTION

We have used the commercial code Fluent for simulating the combustion process in the furnace. A description of the models employed are presented in the next sections.

2.1 Turbulent Flow Field

The model implemented for simulating the turbulent flow was composed by the equation

(5) for the conservation of total mass and the equation (6) for the conservation of momentum in the time averaged form. The Boussinesq's hypothesis was taken into account leading to an effective viscosity given by equation (7). Equation (8) represents the modified total pressure P, considering the contributions due to the turbulent fluctuations.

$$div(\rho \, v) = 0 \tag{5}$$

$$div(\rho \, v \, v) = -grad \, P + div(\mu_{ef} \, grad \, v) + \left[\mu_{ef} (grad \, v)^T\right] \tag{6}$$

$$\mu_{ef} = \mu + \mu_t \tag{7}$$

$$P = p - \frac{2}{3}\left[\mu_{ef} \, div \, v + \rho \, k\right] \tag{8}$$

For calculating the turbulent viscosity it was used the k-ε model of turbulence. In this model, the turbulent viscosity is expressed by the equation (9), where k corresponds to the turbulence kinetic energy and ε corresponds to the dissipation for the turbulence kinetic energy. Equations (10) and (11) represent the conservation for k and ε respectively. Equation (12) represents G, the generation of turbulence kinetic energy.

$$\mu_t = \frac{c_\mu \rho \, k^2}{\varepsilon} \tag{9}$$

$$div(\rho v k) = div\left(\frac{\mu_t}{\mathrm{Pr}_k} \, grad \, k\right) + (G - \rho\varepsilon) \tag{10}$$

$$div(\rho v \varepsilon) = div\left(\frac{\mu_t}{\mathrm{Pr}_\varepsilon} \, grad \, \varepsilon\right) + (c_1 G - c_2 \rho\varepsilon) - \frac{\varepsilon}{k} \tag{11}$$

$$G = \mu_t\left(grad \, v + (grad \, v)^T\right) \circ grad \, v \tag{12}$$

The above equations were solved simultaneously providing results for the turbulent flow field.

2.2 Temperature Field

For simulating the temperature field within the furnace it was solved the equation (13) for the conservation of energy, in which the total enthalpy h is defined as the sum of the enthalpies of each species h_i weighted by its mass fraction m_i, represented by equation (14).

$$div(\rho v h) = div\left[\left(\frac{\mu}{\mathrm{Pr}} + \frac{\mu_t}{\mathrm{Pr}_t}\right) grad \, h\right] + v \bullet grad \, p + S_h \tag{13}$$

$$h = \sum_i m_i h_i \tag{14}$$

Equation (15) represents the enthalpy source S_h due to the chemical reactions and the radiation heat transfer.

$$S_h = S_{reac} + S_{rad} \tag{15}$$

2.3 Chemical Species and Combustion Modeling

For simulating the transport in the gas phase, the mixture was considered as an ideal gas, and a set of conservation equations for the chemical species was solved. Equation (16) represents the conservation for each chemical species.

$$div(\rho v m_i) = div\left[\left(\frac{\mu}{Sc} + \frac{\mu_t}{Sc_t}\right)grad\, m_i\right] + R_i \tag{16}$$

In the above equation, the term R_i represents the source for each species. It may be expressed by the sum of the reaction rates (generation or consumption) for species i in every reaction k, as denoted by $R_{i,k}$ corresponding to equation (17).

$$R_i = \sum_k R_{i,k} \tag{17}$$

The rates in the combustion reactions were calculated by using both the Arrhenius and the Magnussen models (Fluent User's Guide, 1996). In the Arrhenius model, the reaction rate may be computed according to equation (18).

$$R_{i,k} = \eta_{i,k}\, M_i\, T^{\beta_k}\, A_k\, \exp\left(- E_k / RT\right)\prod_j C_j^{\gamma_{j,k}} \tag{18}$$

In the Magnussen model, the rate of reaction is calculated both by equations (19) and (20) and the smallest value is taken (limiting rate). In these expressions, j* represents the reactant which gives the smallest value for $R_{i,k}$, and K_1 and K_2 are empirical constants.

$$R_{i,k} = \eta_{i,k}\, M_i K_1 \rho\, \frac{\varepsilon}{k}\, \frac{m_{j*}}{\eta_{j*,k} M_{j*}} \tag{19}$$

$$R_{i,k} = \eta_{i,k}\, M_i\, K_1\, K_2 \rho\, \frac{\varepsilon}{k}\, \frac{\sum_p m_p}{\sum_p \eta_{p,k}\, M_p} \tag{20}$$

The smallest value obtained in the two models, Arrhenius and Magnussen, was employed as the final value for the reaction rate in the calculation of the source term due to chemical reactions involving species i, R_i.

2.4 Radiation Model

The Discrete Transfer Radiation Model (DTRM) was employed in the computation of the heat fluxes due to radiation. In this model, the change in the radiant intensity I, integrated over

all wavelengths, along a path S, is calculated according to equation (21) when scattering is neglected.

$$\frac{dI}{dS} = -\alpha\,I + \frac{\alpha\,\sigma\,T^4}{\pi} \tag{21}$$

The terms on the right side of equation (21) represent the loss by absorption and the gain by emission due to the participating medium, respectively .

3. PROBLEM SET-UP

3.1 Geometry

The geometry which was simulated, corresponding to a cylindrical combustor, is shown in Figure 1. It was the same geometry used by Garreton (1994) in its experiments. The computational domain was divided into 60 control volumes in the axial direction and 30 control volumes in the radial direction. A non-uniform grid was employed so that high resolution was obtained around the jets and next to the walls.
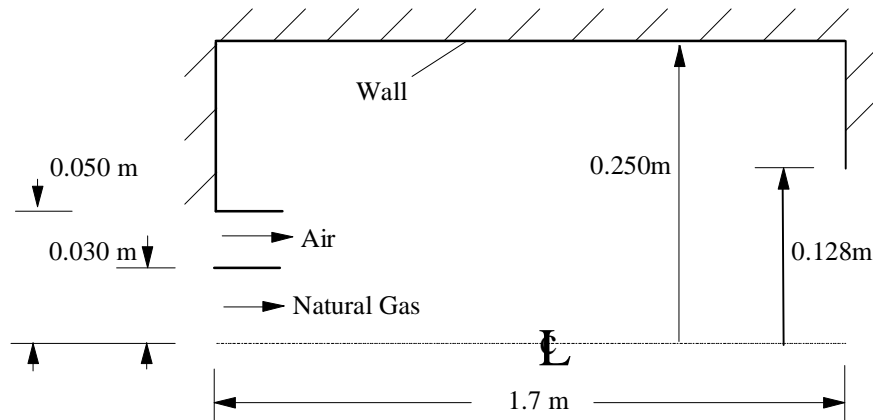

Figure 1 - Schematic of the cylindrical furnace

3.2 Inputs to the Model

The cylindrical combustor, illustrated in Figure 1, may be modeled as axisymmetric, a simplification which was implemented in the burner geometry so that the problem could be treated as two-dimensional.

Natural gas was used as fuel. Taking into consideration that the major component of the natural gas is methane, it was assumed that the combustion reaction taking place inside the furnace could be represented by the equation for the oxidation of methane. The finite rate combustion was modeled using a two steps reaction mechanism (reaction (22) and (23)). The chemical reactions model was represented by reaction (22) and (23) plus reactions (2) and (3) for the NO formation corresponding to the Zeldovich mechanism .

$$CH_4 + \frac{3}{2} O_2 \xrightarrow{k_{22}} CO + 2H_2O \tag{22}$$

$$CO + \frac{1}{2}O_2 \xrightarrow{k_{23}} CO_2 \tag{23}$$

In the NO_x formation mechanism, it was assumed an equilibrium value for the [O] radical concentration, named as $[O]_{equil}$. This value was calculated by using equation (24) from averaged values of temperature and oxygen mole fraction, along a defined flame region. This region corresponds to the highest [O] radical formation rates according to the literature (Isnard & Gomes, 1998), which in turn is a significant precursor species in the NO formation mechanism. Equation (24) corresponds to the partial equilibrium approach (Konnov, 1997) and it accounts for reaction (4).

$$[O]_{equil} = 36.64 T^{1/2}[O_2]^{1/2} \exp(-27123/T) \text{ mol m}^{-3} \tag{24}$$

The NO formation rate was calculated in a postprocessing step, by using only the Arrhenius expression. Because the concentrations of the intermediate radicals (O and N) participating in reactions (2) and (3) are extremely small compared to the stable species, the Magnussen model for the calculation of the reaction rates is limited by these small concentrations, producing unrealistically small results for the NO formation. The Magnussen Model is recommended for global reactions, and not for multi-step reaction mechanisms involving intermediate radicals (Fluent User's Guide 1996).

The parameters used in the reactions calculations are presented in Table 1.

Table 1 - Parameters used in the reactions calculations

Const. Rate	Forward Reaction[a] $\text{m}^3 \text{ kmol}^{-1} \text{ sec}^{-1}$	Reverse Reaction[a] $\text{m}^3 \text{ kmol}^{-1} \text{ sec}^{-1}$
k_2	$6.96 \times 10^{10} \times \exp(-3.159\times10^8/RT)$	1.542×10^{10}
k_3	$1.326 \times 10^7 \, T \times \exp(-2.962\times10^7/RT)$	$3.18 \times 10^6 \, T \times \exp(-1.636\times10^8/RT)$
k_{22}	$2.8 \times 10^{12} \exp(-2.025\times10^8/RT)$	---------
k_{23}	$1.0 \times 10^{15.35} \exp(-1.674\times10^8/RT)$	---------

[a]E_k units, J kmol^{-1}

The considered flame was a turbulent diffusion flame. A nozzle in the center of the combustor introduced natural gas at 0.0125 kg/s. Ambient air entered the combustor coaxially at 0.186 kg/s. The AF ratio is near stoichiometric (about 5% excess fuel). The Reynolds number based on the natural gas jet diameter was approximately 29000.

The natural gas jet was given an inlet temperature of 313K, a methane mass fraction of 0.9, a nitrogen mass fraction of 0.1, a turbulence intensity and length scale of 10% and 0.03m. The air inlet was given a temperature of 323K, oxygen, nitrogen and vapor mass fractions of 0.23, 0.76 and 0.01 respectively, a turbulence intensity and length scale of 6% and 0.04 m.

The constants used in k-ε model were c_1 =1.4, c_2 = 1.9 and c_μ = 0.09. The turbulent Prandtl and Schmidt numbers were set at 0.7. In the Magnussen model the constants K_1 was equal to 4.0 and K_2 was equal to 0.5. The density of the gaseous mixture was calculated by using the ideal gas law, according to equation (25) below, where p_{op} is the average operation pressure inside the furnace. It was assumed that p_{op} was equal to one atmosphere.

$$\rho = \frac{p_{op}}{RT \sum_i m_i / M_i} \qquad (25)$$

In the thermal problem, the heat flux across the furnace wall was prescribed in conformity with values determined in the experiments of Garreton (1994), by measurements of the heat removed by cooling jackets. Table 2 presents the heat flux values on the side walls determined along the combustor. The heat flux was estimated as 26.1 kW/m^2 in the wall close to the jets inlets and 78.9 kW/m^2 in the wall close to the gases exit.

Table 2 – Thermal flux prescribed on the furnace wall

Section	Heat Flux
0 mm < x < 380 mm	26.1 kW/m^2
380 mm < x < 680 mm	39.7 kW/m^2
680 mm < x < 980 mm	59.6 kW/m^2
980 mm < x < 1280 mm	88.3 kW/m^2
1280 mm < x < 1400 mm	95.3 kW/m^2
1400 mm < x < 1700 mm	102.2 kW/m^2

4. RESULTS

Figure 2 shows that the predicted temperature peak reaches 1750 K. Both the trends and the absolute values of the numerical and experimental (Garreton, 1994) results are concordant. A sensitive improvement on the temperature field prediction was obtained by employing this model, in comparison with the last one (Isnard & Gomes, 1998). This progress is due mainly to the two steps combustion model, making it possible to calculate the CO concentrations within the furnace. Throughout comparison with one-step combustion simulations for the same conditions, it could be concluded that the two steps combustion model was responsible for a reduction of 150 K (8%).
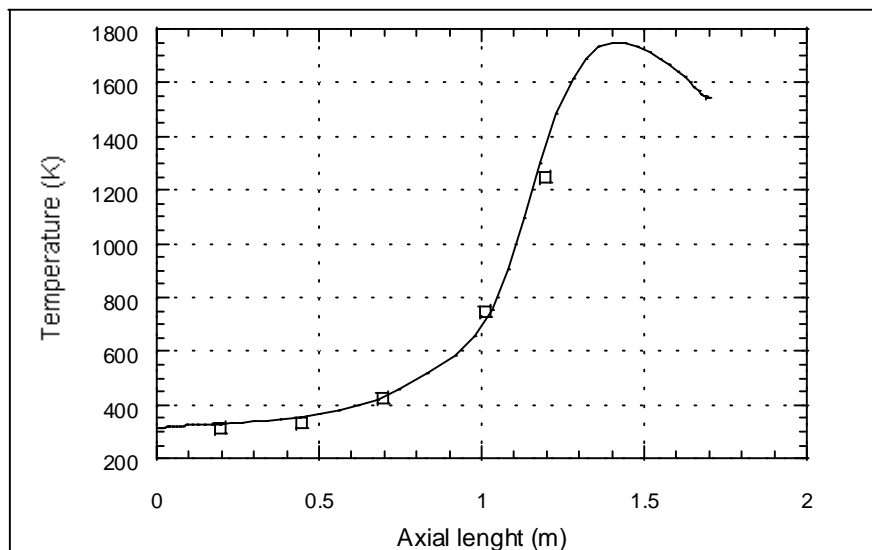

Figure 2 – Comparison between predicted (line) and experimental
(squares) temperature along the symmetry axis of the furnace.

Figures 3 and 4 present respectively the CO and CO_2 mole fractions in the combustor, demonstrating reasonable concordance between predicted and experimental data (Garreton, 1994). In Figure 3, it may be noted that the region corresponding to the maximum CO production and consumption coincides with the region of maximum increase in temperature, indicating that the CO species has an important influence on the temperature field within the furnace. In Figure 4, the highest predicted concentrations of CO_2 are located next to the temperature peak region. As the same way as the temperature field prediction, an evident improvement on the estimate of the chemical species concentrations was obtained by employing this model, in comparison with the previous one (Isnard & Gomes, 1998).
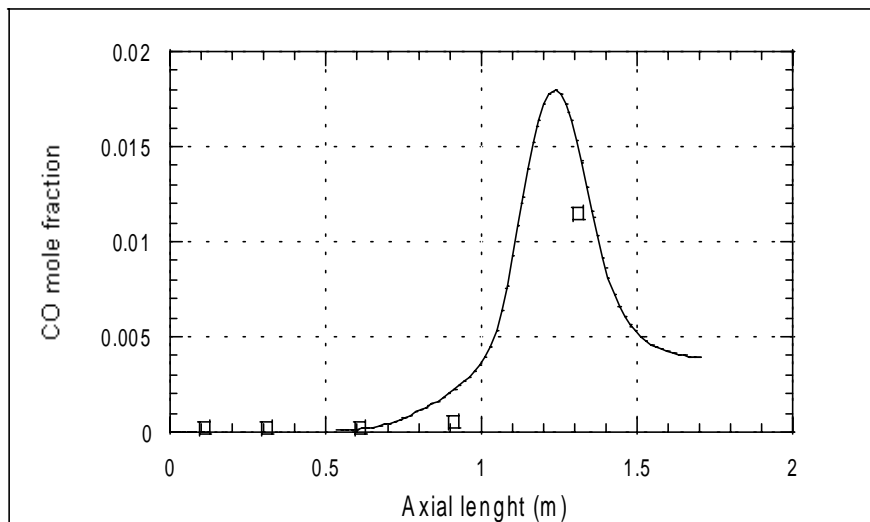

Figure 3 – Comparison between predicted (line) and experimental
(squares) carbon monoxide (CO) mole fraction along the
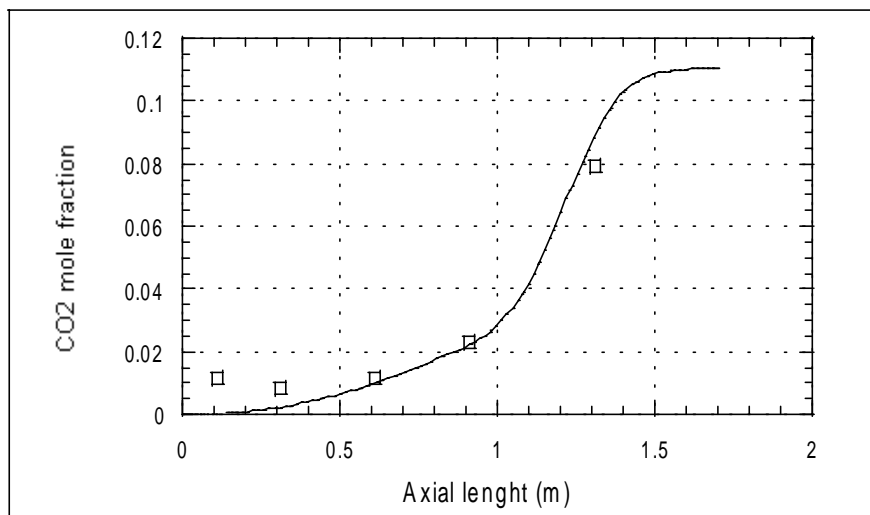symmetry axis of the furnace.

Figure 4 – Comparison between predicted (line) and experimental
(squares) carbon dioxide (CO_2) mole fraction along the
symmetry axis of the furnace.

Figure 5 shows that the peak of NO mole fraction occurs at the exit of the combustor where the combustion reaction has already reached chemical equilibrium. This qualitative result is in accordance to the literature (Seinfeld, 1986) and to the experimental trend. Quantitatively, the predicted NO concentration is unrealistically underestimated in

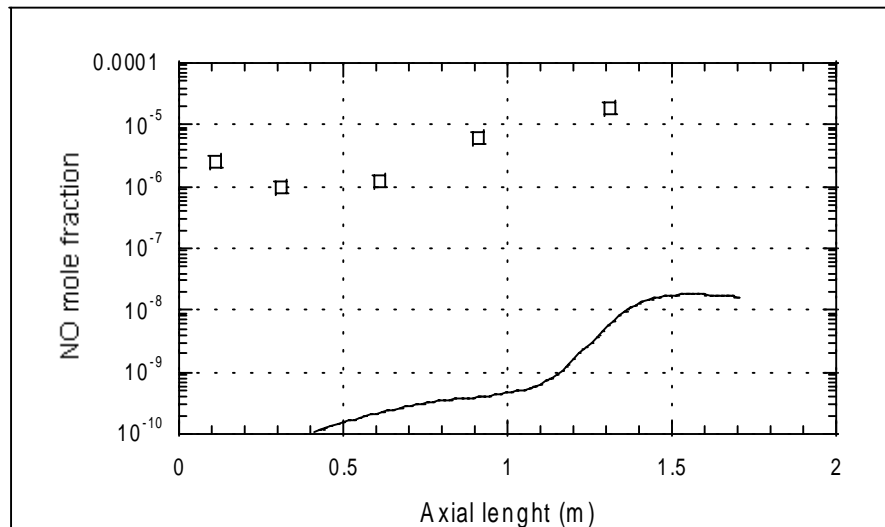comparison with the experimental data of Garreton (1994).

Figure 5 – Comparison between predicted (line) and experimental
(squares) nitric oxide (NO) mole fraction along the
symmetry axis of the furnace.

5. CONCLUSION

The two steps reaction mechanism for combustion modeling influences positively the temperature calculations and produces a good estimate for the CO concentrations within the furnace. The results indicate an important influence of the CO species on the temperature field. The improvement in the temperature field also results in better predictions for the others chemical species like CO_2. The calculated NO concentration levels were unrealistically underestimated in comparison with the experimental data, although the values followed the same trend. In a previous work (Isnard & Gomes ,1998), reasonable predictions for the NO concentration were obtained for temperature levels of about 2300 K, using a thermal mechanism for the NO formation. This may be an indication that the thermal mechanism is more adequate for higher temperature situations than those found in the present work. The low temperatures as well as the excess fuel in the mixture calls for the implementation of the Prompt-NO mechanism together with the Thermal NO for better predictions. More recently, we have obtained more accurate results for the NO concentration field by introducing the PDF model for representing the turbulence-chemistry interaction. Carrying on with this research, others approaches for the prediction of $[O]_{equil}$, as well as more sophisticated models for predicting the NO formation are being implemented and investigated.

6. NOMENCLATURE

A   Pre-exponential Factor
C   Molar Concentration
E   Activation Energy
I   Radiation Intensity
M   Molecular Weight
P   Modified Total Pressure

Pr   Prandtl Number
R   Reaction Rate or Universal Gas Constant
Sc   Schimidt Number
T   Temperature
c_μ Turbulent Viscosity Coefficient

g	Gravity Acceleration		η	Stoichiometric Coefficient
h	Enthalpy		μ	Absolute Viscosity
k	Turbulent Kinetic Energy		ρ	Specific Mass
m	Mass Fraction		σ	Stefan Boltzmann Constant
p	Pressure			
v	Velocity Vector			

Greek Symbols

α Absorption Coefficient

β Temperature Exponent

ε Rate of Dissipation of Turbulent Kinetic Energy or Total emissivity

γ Concentration Exponent

Subscripts

ef Effective Viscosity

i Species

j Reactant Species

k Reaction

p Product Species

t Turbulent Viscosity, Prandlt and Schmidt Numbers

7. REFERENCES

Bowman, Craig T., 1975, "Kinetics of Pollutant Formation and Destruction in Combustion", Progress in Energy Combustion Science.

Bowman, Craig T. and Miller, James A., 1989, "Mechanism and Modeling of Nitrogen Chemistry in Combustion", Progress in Energy Combustion Science.

Chui, E.H., Hughes, P.M.J. and Mueller, C.M., 1997, "Prediction and Measurement of NO_x and Combustion Characteristics in Two Natural Gas Flames", Fourth International Conference on Technologies and Combustion for a Clean Environment, Lisboa , Portugal.

Fluent User's Guide, version 4.3, Fluent Incorporated, New Hampshire, March 1995.

Garreton, D., Simonin, 1994, First Workshop on Aerodynamics of Steady State Combustion Chambers and Furnaces: Final Results, Chatou, France.

Gomes, Marcos S. P., Nieckele, Angela O., Naccache, Monica F. and Kobayashi, William T., 1997, "Numerical Investigation of the Oxygen Enriched Combustion Process in a Cylindrical Furnace", Fourth International Conference on Technologies and Combustion for a Clean Environment, Lisboa , Portugal.

Isnard, A, Gomes, M.S.P., 1998, Numerical Investigations on the NO_x Formation in Natural Gas Combustion, 7th Brazillian Congress of Engineering and Thermal Sciences, Rio de Janeiro, Brasil.

Konnov, A.A., 1997, "NO Formation Rates in Natural Gas Combustion", Fourth International Conference on Technologies and Combustion for a Clean Environment, Lisboa, Portugal.

Magel, H. C., Schnell,U. and Hein, K.R.G., 1996, "Modelling of Hydrocarbon and Nitrogen Chemistry in Turbulent Combustor Flows Using Detailed Reactions Mechanisms", 3rd Workshop on Modelling of Chemical Reaction Systems, Heidelberg.

Patankar, S.V., 1980, Numerical Heat Transfer and Fluid Flow. Hemisphere Publishing Corporation, New York.

Seinfeld's, John H., 1986, Atmospheric Chemistry and Physics of Air Pollution, John Wiley & Sons, New York.

Tomeczek, J. and Gradón,B, 1997, "The Rate of Nitric Oxide Formation in Hydrocarbon Flames", Fourth International Conference on Technologies and Combustion for a Clean Environment, Lisboa, Portugal.